

# Capacity of Sparse Multipath Channels in the Ultra-Wideband Regime

Vasanthan Raghavan\*, Gautham Hariharan and Akbar M. Sayeed

**Abstract**—This paper studies the ergodic capacity of time- and frequency-selective multipath fading channels in the ultrawideband (UWB) regime when training signals are used for channel estimation at the receiver. Motivated by recent measurement results on UWB channels, we propose a model for sparse multipath channels. A key implication of sparsity is that the independent degrees of freedom (DoF) in the channel scale sub-linearly with the signal space dimension (product of signaling duration and bandwidth). Sparsity is captured by the number of resolvable paths in delay and Doppler. Our analysis is based on a training and communication scheme that employs signaling over orthogonal short-time Fourier (STF) basis functions. STF signaling naturally relates sparsity in delay-Doppler to coherence in time-frequency. We study the impact of multipath sparsity on two fundamental metrics of spectral efficiency in the wideband/low-SNR limit introduced by Verdu: first- and second-order optimality conditions. Recent results by Zheng *et. al.* have underscored the large gap in spectral efficiency between coherent and non-coherent extremes and the importance of channel learning in bridging the gap. Building on these results, our results lead to the following implications of multipath sparsity: 1) The coherence requirements are shared in both time and frequency, thereby significantly relaxing the required scaling in coherence time with SNR; 2) Sparse multipath channels are asymptotically coherent — for a given but large bandwidth, the channel can be learned perfectly and the coherence requirements for first- and second-order optimality met through sufficiently large signaling duration; and 3) The requirement of peaky signals in attaining capacity is eliminated or relaxed in sparse environments.

## I. INTRODUCTION

Emerging applications of ultrawideband (UWB) radio technology have inspired both academic and industrial research on wide-ranging problems. The large bandwidth of UWB systems results in fundamentally new channel characteristics as evident from recent measurement campaigns [1], [2], [3]. This is due to the fact that, analogous to radar, wideband waveforms enable multipath resolution in delay at a much finer scale – delay resolution increases in direct proportion to bandwidth. From a communication-theoretic perspective, the number of resolvable multipath components reflects the

number of independent degrees of freedom (DoF) in the channel [4], [5], which in turn governs fundamental limits on performance. When the channel coefficients corresponding to resolvable multipath are perfectly known at the receiver (coherent regime), the DoF reflect the level of delay-Doppler diversity afforded by the channel [4], [6]. On the other hand, when the channel coefficients are unknown at the receiver (non-coherent regime), the DoF reflect the level of uncertainty in the channel. The fundamental limits to communication, such as capacity, can be radically different in the coherent and non-coherent extremes, and communication schemes that explicitly or implicitly learn the channel can bridge the gap between the extremes [7], [8].

In this paper, we study the ergodic capacity of time- and frequency-selective UWB channels in the non-coherent regime where the channel is explicitly estimated at the receiver using training signals. Motivated by recent measurement results, our focus is on channels that exhibit *sparse* multipath – the number of DoF in the channel scale *sub-linearly* with the signal space dimension (product of signaling duration and bandwidth) – in contrast to the widely prevalent assumption of rich multipath in which the number of DoF scale linearly with signal space dimension. Whether a multipath channel is rich or sparse depends on the operating frequency, bandwidth and the scattering environment [1]. For example, [2] reports rich channels even for 7.5 GHz bandwidth in industrial environments whereas [3] reports sparse multipath in residential environments at the same bandwidth. Overall, large bandwidths increase the likelihood of channel sparsity [1], [9]. In time-selective scenarios, the likelihood of sparsity is increased further due to multipath resolution in Doppler.

The results in this paper build on two recent works that explore ergodic capacity of fading channels in the wideband/low-SNR regime [7], [8]. The seminal work in [7] shows that spectral efficiency in the wideband regime is captured by two fundamental metrics:  $\frac{E_b}{N_o \min}$ , the minimum energy per bit for reliable communication, and  $S_0$ , the wideband slope. A signaling scheme that achieves  $\frac{E_b}{N_o \min}$  is termed *first-order optimal* and one that achieves  $S_0$  as well is termed *second-order optimal*. The results of [7] also show that knowledge of channel state information (CSI) at the receiver imposes a sharp cut-off on the achievability of ergodic capacity in the wideband regime. In particular, while QPSK signaling is second-order optimal when perfect CSI is available (coherent regime), flash (peaky) signaling is necessary for first-order optimality when no CSI is available (non-coherent regime). However, a flash signaling scheme, besides having an unbounded peak-to-average ratio (and hence practically infeasible), also results in

Manuscript received XXXX; revised XXXX. This work was supported in part by the National Science Foundation under Grant CCF-0431088. This paper was presented in part at the 43rd Allerton Conference (Allerton 2005), Monticello, IL and at the 14th Adaptive Sensor Array Processing Workshop (ASAP 2006), Cambridge, MA. The associate editor coordinating the review of this manuscript and approving it for publication was Dr. Michael L. Honig.

V. Raghavan is with the Department of Electrical and Computer Engineering, University of Illinois, Urbana-Champaign, Urbana, IL 61801 USA (email: vasanthan\_raghavan@iee.org).

G. Hariharan and A. M. Sayeed are with the Department of Electrical and Computer Engineering, University of Wisconsin, Madison, WI 53706 USA (email: gauthamh@cae.wisc.edu, akbar@enr.wisc.edu).

$S_0 = 0$  and thereby violating second-order optimality.

This apparent sharp cut-off in the peak-to-average ratio of capacity achieving signaling schemes between the coherent and non-coherent extremes was examined in [8]. If the coherence time of the channel scales at a sufficiently fast rate with the bandwidth, Zheng *et al.* show that a communication scheme with explicit training can bridge the gap between the two extremes. However, no physical justification is provided for the existence of such a scaling in coherence time with bandwidth. In other related work, [10] investigates the effect of channel uncertainty when using spread-spectrum signals. They conclude that the number of resolvable channel paths need to scale sub-linearly with bandwidth in order to achieve the wideband limit (first-order optimality in [7]).

We first propose a model for sparse multipath channels to capture the physical channel characteristics in the UWB regime as observed in recent measurement studies. In a time- and frequency-selective environment, multipath components can be resolved in delay and Doppler where the resolution in delay/Doppler increases with signaling bandwidth/duration [5]. A key implication of multipath sparsity is that the number of DoF in the channel (resolvable delay-Doppler coefficients) scales sub-linearly with the signal space dimension. Our analysis of the ergodic capacity of doubly-selective UWB channels is based on signaling over short-time Fourier (STF) basis functions [11], [6] that are a generalization of OFDM signaling and serve as approximate eigenfunctions for underspread channels. Furthermore, STF signaling naturally relates multipath sparsity in delay-Doppler to coherence or correlation in time and frequency [6]. We consider a communication scheme in which explicit training symbols are used to estimate the channel at the receiver. The capacity of this scheme is then studied to investigate the impact of multipath sparsity on achieving coherent capacity.

The results of this paper lead to several new contributions and insights on the impact of sparsity. First, we show that multipath sparsity provides a natural physical mechanism for scaling of coherence time,  $T_{coh}$ , with bandwidth/SNR, as assumed in [8]. Second, the coherence requirements for achieving capacity are shared between both time and frequency: the coherence bandwidth,  $W_{coh}$ , increases with bandwidth,  $W$  (due to sparsity in delay), and the coherence time,  $T_{coh}$ , increases with signaling duration  $T$  (due to sparsity in Doppler). As a result, the scaling requirements on  $T_{coh}$  with  $W$  (or  $\text{SNR} = P/W$ , where  $P$  is the total transmit power) needed in [8] for first- and second-order optimality are replaced by scaling requirements on the time-frequency coherence dimension  $N_{coh} = T_{coh}W_{coh}$ . This leads to significantly relaxed requirements on  $T_{coh}$  scaling with bandwidth/SNR compared to those in [8]. Third, we show that sparse multipath channels are *asymptotically coherent*; that is, for a sufficiently large but fixed bandwidth, the conditions for first- and second-order optimality can be achieved simply by making the signaling duration sufficiently large. We quantify the required (power-law) scaling in  $T$  with  $W$  for first- and second-order optimality as a function of channel sparsity. This asymptotic coherence of sparse channels is also manifested in the performance of the training scheme – consistent chan-

nel estimation is achieved with vanishing fraction of energy expended on training. The asymptotic coherence of sparse channels also eliminates/relaxes the need for peaky signaling that has been emphasized in existing results [12], [7] on non-coherent capacity, implicitly based on a rich multipath assumption. We discuss how sparsity and peakiness can be traded off suitably depending on system design requirements. Finally, the results in this paper are shown to hold in general, independent of the type of scaling laws used to model sparsity.

The paper is organized as follows. The system setup, including the sparse channel model and training-based STF signaling scheme, is described in Section II. In Section III, we study the ergodic capacity of sparse channels with perfect CSI and for the training-based communication scheme. A discussion of the results, including their relation to existing work is provided in Section IV. Numerical results are provided to illustrate the implications of the theoretical results. Concluding remarks and directions for future work are discussed in Section V.

## II. SYSTEM SETUP

In this section, we first propose a model for sparse multipath channels in terms of the number of paths that are resolvable in delay and Doppler. We then develop a system model based on orthogonal short-time Fourier (STF) signaling and propose a block fading channel model that naturally relates multipath sparsity in delay-Doppler to coherence in time-frequency. We then describe the training-based communication scheme in the STF domain whose capacity is investigated in this paper.

### A. Sparse Multipath Channel Modeling

We consider a single-user single-antenna communication system in complex baseband

$$y(t) = \int_0^{T_m} \int_{-\frac{W_d}{2}}^{\frac{W_d}{2}} h(\tau, \nu) x(t - \tau) e^{j2\pi\nu t} d\nu d\tau + w(t) \quad (1)$$

where the channel is characterized by the delay-Doppler spreading function,  $h(\tau, \nu)$ , and  $x(t)$ ,  $y(t)$  and  $w(t)$  represent the transmitted, received and additive white Gaussian noise (AWGN) waveforms, respectively.  $T_m$  and  $W_d$  represent the delay and Doppler spreads of the channel. We assume an underspread channel,  $T_m W_d \ll 1$ , which is valid for most radio channels. A physical discrete multipath channel can be modeled as

$$\begin{aligned} h(\tau, \nu) &= \sum_n \beta_n \delta(\tau - \tau_n) \delta(\nu - \nu_n) \\ y(t) &= \sum_n \beta_n x(t - \tau_n) e^{j2\pi\nu_n t} + w(t) \end{aligned} \quad (2)$$

where  $\beta_n$ ,  $\tau_n \in [0, T_m]$  and  $\nu_n \in [-W_d/2, W_d/2]$  denote the complex path gain, delay and Doppler shift associated with the  $n$ -th path. Note that the above model assumes that the carrier frequency is much larger than the signaling bandwidth so that the effects of motion are accurately captured via Doppler shifts (the shrinking or dilation of the signaling waveforms is ignored).

The physical model (2), while accurate, is complex to analyze from a communication-theoretic perspective due to

the non-linear dependence on propagation parameters  $\tau_n$  and  $\nu_n$ . We instead use a linear *virtual representation* [5], [4] for time- and frequency-selective multipath channels that captures the channel characteristics in terms of *resolvable paths* and greatly facilitates analysis. Throughout the paper, we consider signaling over a duration  $T$  and (two-sided) bandwidth  $W$ . The virtual representation, illustrated in Fig. 1(a), uniformly samples the multipath in delay and Doppler at a resolution commensurate with  $W$  and  $T$ , respectively [5], [4]

$$y(t) = \sum_{\ell=0}^L \sum_{m=-M}^M h_{\ell,m} x(t - \ell/W) e^{j2\pi m t/T} \quad (3)$$

$$h_{\ell,m} \approx \sum_{n \in S_{\tau,\ell} \cap S_{\nu,m}} \beta_n \quad (4)$$

where  $L = \lceil T_m W \rceil$ ,  $M = \lceil T W_d / 2 \rceil$ ,  $S_{\tau,\ell} = \{n : \ell/W - 1/2W < \tau_n \leq \ell/W + 1/2W\}$  denotes the set of all paths whose delays lie within the delay resolution bin of width  $\Delta\tau = 1/W$  centered around the  $\ell$ -th resolvable (virtual) delay,  $\hat{\tau} = \ell/W$ , and  $S_{\nu,m} = \{n : m/T - 1/2T < \nu_n \leq m/T + 1/2T\}$  denotes the set of all paths whose Doppler shifts lie within the Doppler resolution bin of width  $\Delta\nu = 1/T$  centered around the  $m$ -th resolvable (virtual) Doppler shift,  $\hat{\nu}_m = m/T$ . The sampled representation (3) is linear and is characterized by the virtual delay-Doppler channel coefficients  $\{h_{\ell,m}\}$ . The expression (4) states that the channel coefficient  $h_{\ell,m}$  consists of the sum of gains of all paths whose delays and Doppler shifts lie within the  $(\ell, m)$ -th delay-Doppler resolution bin of width  $\Delta\tau \times \Delta\nu$  centered around the sampling point  $(\hat{\tau}, \hat{\nu}_m) = (\ell/W, m/T)$  in the  $(\tau, \nu)$  (delay-Doppler) space. It follows that *distinct*  $h_{\ell,m}$ 's correspond to approximately<sup>1</sup> *disjoint* subsets of paths and are hence approximately statistically independent (due to independent path phases). This approximation gets more accurate with increasing  $T$  and  $W$ , due to higher delay-Doppler resolution, and we assume that the channel coefficients  $\{h_{\ell,m}\}$  are perfectly independent. We also assume Rayleigh fading in which  $\{h_{\ell,m}\}$  are zero-mean Gaussian random variables.<sup>2</sup> Thus, for Rayleigh fading, the channel statistics are characterized by the power in the virtual channel coefficients

$$\Psi(\ell, m) = E[|h_{\ell,m}|^2] \approx \sum_{n \in S_{\tau,\ell} \cap S_{\nu,m}} E[|\beta_n|^2]. \quad (5)$$

We define *dominant non-zero channel coefficients*,  $h_{\ell,m}$ 's, as those which contribute significant channel power; that is, the coefficients for which  $\Psi(\ell, m) > \gamma$  for some prescribed threshold  $\gamma > 0$ .<sup>3</sup> In Fig. 1(a), the delay-Doppler resolution bins with a dot in them represent the dominant channel coefficients. Let  $D$  denote the number of dominant non-zero channel coefficients; that is,  $D = |\{(\ell, m) : \Psi(\ell, m) > \gamma\}|$ . The parameter  $D$  reflects the (dominant) statistically independent degrees of freedom (DoF) in the channel and also signifies the delay-Doppler diversity afforded by the channel. Furthermore,

<sup>1</sup>Approximate due to finite  $T$  and  $W$ .

<sup>2</sup>This would be true if, for example, there are sufficiently large number of *unresolvable* paths contributing to each  $h_{\ell,m}$  in (4).

<sup>3</sup>The choice of the threshold  $\gamma$  depends on the operating SNR and discussion of the choice of this threshold is beyond the scope of this paper.

we decompose  $D$  as  $D = D_T D_W$  where  $D_T$  denotes the Doppler/time diversity and  $D_W$  the frequency/delay diversity. The channel DoF or delay-Doppler diversity is bounded as:

$$D = D_T D_W \leq D_{\max} = D_{T,\max} D_{W,\max} \\ D_{T,\max} = \lceil T W_d \rceil, \quad D_{W,\max} = \lceil T_m W \rceil \quad (6)$$

where  $D_{T,\max}$  denotes the maximum number of resolvable paths in Doppler (maximum Doppler/time diversity) and  $D_{W,\max}$  denotes maximum number of resolvable paths in delay (maximum delay/frequency diversity). Note that  $D_{T,\max}$  and  $D_{W,\max}$  increase linearly with  $T$  and  $W$ , respectively.  $D = D_{\max}$  represents a rich multipath environment in which each resolution bin in Fig. 1(a) corresponds to a dominant channel coefficient.

However, from recent measurement campaigns [1], [13], [14] for UWB channels, there is growing experimental evidence that the dominant channel coefficients get sparser in delay as the bandwidth increases. Most existing measurement results are for indoor UWB channels and do not consider the effect of Doppler. We are interested in modeling scenarios with Doppler effects, as well, due to motion. In such cases, as we consider large bandwidths and/or long signaling durations, the resolution of paths in both delay and Doppler domains gets finer, leading to the scenario in Fig. 1(a) where the delay-Doppler resolution bins are sparsely populated with paths, i.e.  $D < D_{\max}$ .

We formally model multipath sparsity with a *sub-linear* scaling in  $D_T$  and  $D_W$  with  $T$  and  $W$ :

$$D_T \sim (T W_d)^{\delta_1}, \quad D_W \sim (T_m W)^{\delta_2}, \quad \delta_1, \delta_2 \in [0, 1] \quad (7)$$

where the smaller the value of  $\delta_i$ , the slower (sparser) the growth in the resolvable paths in the corresponding domain. Note that this directly implies that the total number of delay-Doppler DoF,  $D = D_T D_W$ , scales sub-linearly with the number of signal space dimensions  $N = T W$ .

*Remark 1:* We focus on the power-law scaling in (7) as a concrete example for studying the impact of sparsity on capacity. As discussed in Sec. IV-F, the results of this paper hold true for arbitrary sub-linear scaling laws.

*Remark 2:* With perfect CSI at the receiver, the parameter  $D$  denotes the delay-Doppler diversity afforded by the channel, whereas with no CSI, it reflects the level of channel uncertainty; the number of channel parameters that need to be estimated for coherent processing at the receiver.

## B. Orthogonal Short-Time Fourier Signaling

We consider signaling using an orthonormal short-time Fourier (STF) basis [6], [11] that is a natural generalization of orthogonal frequency-division multiplexing (OFDM) for time-varying channels.<sup>4</sup> An orthogonal STF basis for the signal space is generated from a fixed prototype waveform  $g(t)$  via time and frequency shifts:  $\phi_{\ell m}(t) = g(t - \ell T_o) e^{j2\pi W_o t}$ , where  $T_o W_o = 1$ ,  $\ell = 0, \dots, N_T - 1$ ,  $m = 0, \dots, N_W - 1$  and

<sup>4</sup>STF signaling can be considered as OFDM signaling over a block of OFDM symbol periods and with an appropriately chosen OFDM symbol duration.

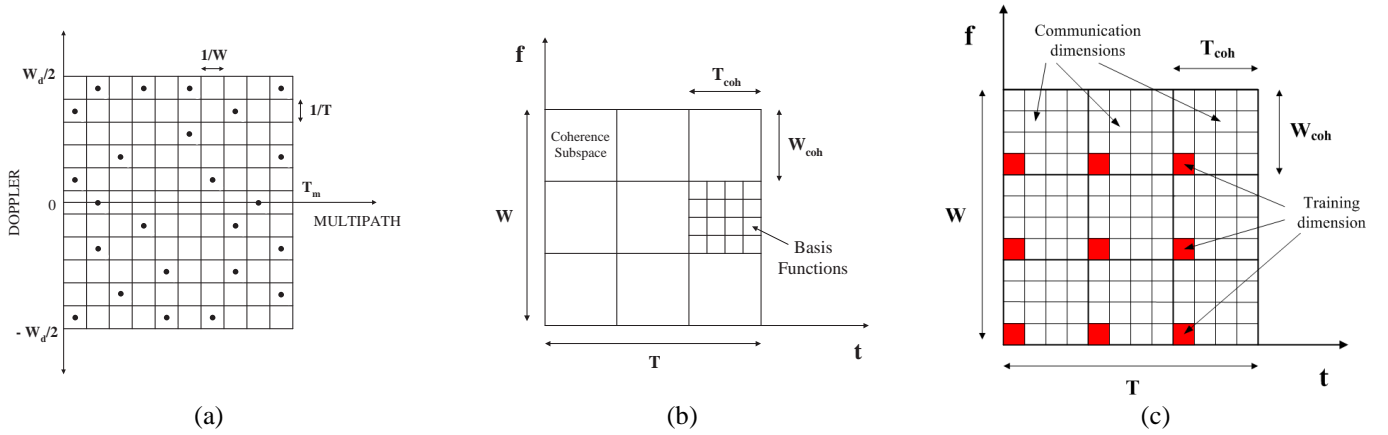


Fig. 1. (a) Delay-doppler sampling commensurate with signaling duration and bandwidth. (b) Time-frequency coherence subspaces in STF signaling. (c) Illustration of the training-based communication scheme in the STF domain. One dimension in each coherence subspace (dark squares) represents the training dimension and the remaining dimensions are used for communication.

$N = N_T N_W = TW$  with  $N_T = T/T_o$ ,  $N_W = W/W_o$ . The transmitted signal can be represented as

$$x(t) = \sum_{\ell=0}^{N_T-1} \sum_{m=0}^{N_W-1} x_{\ell m} \phi_{\ell m}(t) \quad 0 \leq t \leq T \quad (8)$$

where  $\{x_{\ell m}\}$  represent the  $N$  transmitted symbols that are modulated onto the STF basis waveforms. At the receiver, the received signal is projected onto the STF basis waveforms to yield the received symbols

$$y_{\ell m} = \langle y, \phi_{\ell m} \rangle = \sum_{\ell', m'} h_{\ell m, \ell' m'} x_{\ell' m'} + w_{\ell m}. \quad (9)$$

We can represent the system using an  $N$ -dimensional matrix equation

$$\mathbf{y} = \sqrt{\text{SNR}} \mathbf{H} \mathbf{x} + \mathbf{w} \quad (10)$$

where  $\mathbf{w}$  represents the additive noise vector whose entries are i.i.d.  $\mathcal{CN}(0, 1)$ . The  $N \times N$  matrix consists of the channel coefficients  $\{h_{\ell m, \ell' m'}\}$  in (9). The parameter SNR represents the transmit energy per modulated symbol and for a given transmit power  $P$  equals  $\text{SNR} = \frac{TP}{TW} = \frac{P}{W}$ . In this work, our focus is on the UWB regime, where  $\text{SNR} \rightarrow 0$  as  $W \rightarrow \infty$  for a fixed  $P$ .

For sufficiently underspread channels, the parameters  $T_o$  and  $W_o$  can be matched to  $T_m$  and  $W_d$  so that the STF basis waveforms serve as approximate eigenfunctions of the channel [11], [6]; that is, (9) simplifies to<sup>5</sup>  $y_{\ell m} \approx h_{\ell m} x_{\ell m} + w_{\ell m}$ . Thus the  $N \times N$  channel matrix  $\mathbf{H}$  is approximately diagonal. In this work, we assume that  $\mathbf{H}$  is exactly diagonal; that is,

$$\mathbf{H} = \text{diag} \left[ \underbrace{h_{11} \cdots h_{1N_c}}_{\text{Subspace 1}}, \underbrace{h_{21} \cdots h_{2N_c}}_{\text{Subspace 2}}, \cdots, \underbrace{h_{D1} \cdots h_{DN_c}}_{\text{Subspace } D} \right]. \quad (11)$$

The diagonal entries of  $\mathbf{H}$  in (11) also admit an intuitive block fading interpretation in terms of *time-frequency coherence subspaces* [6] illustrated in Fig. 1(b). The signal space is partitioned as  $N = TW = N_c D$  where  $D$  represents the number of statistically independent time-frequency coherence

subspaces, reflecting the DoF in the channel or the delay-Doppler diversity (see (6)), and  $N_c$  represents the dimension of each coherence subspace, which we refer to as the **coherence dimension**. In the block fading model in (11), the channel coefficients over the  $i$ -th coherence subspace  $h_{i1}, \dots, h_{iN_c}$  are assumed to be identical,  $\{h_i\}$ , whereas the coefficients across different coherence subspaces are independent. Furthermore, due to the stationarity of the channel statistics across time and frequency, the different  $h_i$  are identically distributed. Thus, the  $D$  distinct STF channel coefficients,  $\{h_i\}$ , corresponding to the  $D$  independent coherence subspaces, are i.i.d. zero-mean Gaussian random variables (Rayleigh fading). The variance of each channel coefficient is equal to  $\mathbf{E}[|h_i|^2] = \sum_n \mathbf{E}[|\beta_n|^2]$  which we normalize to unity [6].

Using the DoF scaling for sparse channels in (7), the coherence dimension can be computed as

$$T_{coh} = \frac{T}{D_T} = T^{1-\delta_1} / W_d^{\delta_1} \quad (12)$$

$$W_{coh} = \frac{W}{D_W} = W^{1-\delta_2} / T_m^{\delta_2} \quad (13)$$

$$N_c = T_{coh} W_{coh} = \frac{T^{1-\delta_1}}{W_d^{\delta_1}} \frac{W^{1-\delta_2}}{T_m^{\delta_2}} \geq \left\lceil \frac{1}{T_m W_d} \right\rceil \quad (14)$$

where  $T_{coh}$  is the *coherence time* and  $W_{coh}$  is the *coherence bandwidth* of the channel, as illustrated in Fig. 1(b). Note that  $\delta_1 = \delta_2 = 1$  corresponds to a rich multipath channel in which  $N_c = 1/(T_m W_d)$  is *constant* and  $D = D_{\max}$  increases *linearly* with  $N = TW$ . This is the assumption prevalent in existing works. In contrast, for sparse channels,  $(\delta_1, \delta_2) \in (0, 1)$ , and both  $N_c$  and  $D$  increase *sub-linearly* with  $N$ .

The coherence dimension plays a key role in our analysis. In terms of channel parameters,  $N_c$  increases with decreasing  $T_m W_d$  as well as with smaller  $\delta_i$ . In terms of signaling parameters,  $N_c$  can be increased by increasing  $T$  and/or  $W$ . On the other hand, when the channel is rich,  $N_c$  depends only on  $T_m W_d$  and does not scale with  $T$  or  $W$ .

Using (13), we note that

$$W_{coh} = \frac{W^{1-\delta_2}}{(T_m)^{\delta_2}} = \frac{P^{1-\delta_2}}{(T_m)^{\delta_2} \text{SNR}^{1-\delta_2}} \quad (15)$$

<sup>5</sup>The STF channel coefficients are different from the delay-Doppler coefficients, even though we are using the same symbols.

and thus  $W_{coh}$  naturally scales with SNR. Using (15), the expression for  $N_c$  in (14) becomes

$$N_c = \frac{T^{1-\delta_1}}{(W_d)^{\delta_1}} \frac{P^{1-\delta_2}}{(T_m)^{\delta_2} \text{SNR}^{1-\delta_2}}. \quad (16)$$

Our focus is on computing the sparse channel capacity and as we will see later in Section III, capacity turns out to be a function only of the parameters  $N_c$  and SNR. Furthermore, the following relation between  $N_c$  and  $\text{SNR} = P/W$  plays a key role in our analysis

$$N_c = \frac{1}{\text{SNR}^\mu}, \quad \mu > 0, \quad (17)$$

where the parameter  $\mu$  reflects the level of channel coherence. Equating (17) with (16) leads to the following canonical relationship

$$T = \frac{(T_m^{\delta_2} W_d^{\delta_1})^{\frac{1}{1-\delta_1}} W^{\frac{\mu-1+\delta_2}{1-\delta_1}}}{P^{\frac{\mu}{1-\delta_1}}} \quad (18)$$

that relates the signaling parameters  $(T, W, P)$ , as a function of the channel parameters, in order to satisfy (17). Equations (17) and (18) are the two key equations that capture the impact of sparsity and we will revisit them in Section IV. We next describe the training-based communication scheme in the STF domain that serves as the workhorse of the capacity analysis in this paper.

### C. Training-Based Communication Using STF Signaling

Our interest is primarily in the non-coherent scenario when there is no CSI at the receiver *a priori*. We focus on a communication scheme in which the transmitted signals include training symbols to enable channel estimation and coherent detection. Although it is argued in [8], [15] that training-based schemes are sub-optimal from a capacity point of view, the restriction to training schemes is motivated by practical considerations. We assume that both the transmitter and the receiver have knowledge of channel statistics (values of  $T_m$ ,  $W_d$ ,  $\delta_1$  and  $\delta_2$  in our model).

We now describe the training-based communication scheme, adapted from [8] to STF signaling. The total energy available for training and communication is  $PT$ , of which a fraction  $\eta$  is used for training and the remaining fraction  $(1-\eta)$  is used for communication. Since the quality of the channel estimate over one coherence subspace depends only on the training energy and *not* on the number of training symbols [15], our scheme uses one signal space dimension in each coherence subspace for training and the remaining  $(N_c - 1)$  for communication, as illustrated in Fig. 1(c). We consider minimum mean squared error (MMSE) channel estimation and the two metrics that capture channel estimation performance are (i)  $\eta$ , the fraction of energy used for estimation, and (ii) MSE, the mean squared error in estimating each channel coefficient.

The training energy to estimate the channel coefficient in one coherence subspace is given by

$$E_{tr} = \frac{\eta TP}{D} \stackrel{(a)}{=} \eta N_c \text{SNR} \quad (19)$$

where (a) follows from the fact that  $\text{SNR} = \frac{P}{W}$  and  $N_c D = TW$ . Recall that  $N = N_c D = TW = N_T N_W$  and  $D = D_T D_W$ . Similarly we partition  $N_c = N_{c,T} N_{c,W}$  where  $N_{c,T} = N_T / D_T$  is the temporal coherence dimension and  $N_{c,W} = N_W / D_W$  is the spectral coherence dimension and represent the number of STF basis functions that lie within  $T_{coh}$  and  $W_{coh}$ , respectively (see Fig. 1(c)). The following equations describe training in the STF system:

$$\begin{aligned} y_{\ell m} &= \sqrt{E_{tr}} h_{\ell m} x_{\ell m} + w_{\ell m}, \\ \ell &= (i-1)N_{c,T} + 1, \quad m = (j-1)N_{c,W} + 1, \\ i &= 1, \dots, D_T, \quad j = 1, \dots, D_W \end{aligned} \quad (20)$$

where  $\{x_{\ell m}\}$  are the  $D$  training symbols (with  $|x_{\ell m}|^2 = 1$ ) known at the receiver that are used to estimate the  $D$  channel coefficients  $\{h_{\ell m}\}$  with  $\mathbf{E}[|h_{\ell m}|^2] = 1$ .

The communication energy per transmitted data symbol is given by  $E_{cm} = \frac{(1-\eta)TP}{(N_c-1)D} = \frac{(1-\eta)N_c \text{SNR}}{(N_c-1)}$ . The communication component of the system can be described by

$$\begin{aligned} y_{\ell' m'} &= \sqrt{E_{cm}} h_{\ell' m'} x_{\ell' m'} + w_{\ell' m'}, \\ \ell' &= (i-1)N_{c,T} + 2, \dots, iN_{c,T} \\ m' &= (j-1)N_{c,W} + 2, \dots, jN_{c,W}, \\ i &= 1, \dots, D_T, \quad j = 1, \dots, D_W \end{aligned} \quad (21)$$

where  $\{x_{\ell' m'}\}$  now represent the  $(N_c - 1)D$  communication symbols with  $\mathbf{E}[|x_{\ell' m'}|^2] = 1$ . We can rewrite (21) as

$$y_{\ell' m'} = \sqrt{E_{cm}} \hat{h}_{\ell' m'} x_{\ell' m'} + \sqrt{E_{cm}} \Delta_{\ell' m'} x_{\ell' m'} + w_{\ell' m'} \quad (22)$$

and  $\hat{h}_{\ell' m'}$  is the MMSE estimate of  $h_{\ell' m'}$  and is given by

$$\hat{h}_{\ell' m'} = \frac{\sqrt{E_{tr}}}{1 + E_{tr}} y_{\ell' m'} x_{\ell' m'}^*$$

and  $\Delta_{\ell' m'} = h_{\ell' m'} - \hat{h}_{\ell' m'}$  is the error in the estimate. The resulting MSE is given by

$$\begin{aligned} \text{MSE}(\eta, N_c, \text{SNR}) &= \mathbf{E} \left[ |h_{\ell' m'} - \hat{h}_{\ell' m'}|^2 \right] \\ &= \mathbf{E} \left[ |\Delta_{\ell' m'}|^2 \right] \\ &= \frac{1}{1 + E_{tr}} = \frac{1}{1 + \eta N_c \text{SNR}}. \end{aligned} \quad (23)$$

We are now ready to compute the ergodic capacity of the training-based communication system.

### III. ERGODIC CAPACITY OF THE TRAINING-BASED COMMUNICATION SCHEME

We first characterize the coherent capacity of the wideband channel with perfect CSI at the receiver which serves as a benchmark. The coherent capacity per dimension (in bps/Hz) is

$$C_{coh}(\text{SNR}) = \sup_{\mathbf{Q}: \text{Tr}(\mathbf{Q}) \leq TP} \frac{\mathbf{E} \left[ \log_2 \det (\mathbf{I}_{N_c D} + \mathbf{H} \mathbf{Q} \mathbf{H}^H) \right]}{N_c D} \quad (24)$$

where  $P$  denotes transmit power and  $\mathbf{H}$  is the diagonal, block-fading channel matrix in (11). The optimization is over the set of positive semi-definite transmit covariance matrices  $\mathbf{Q}$ . Due

to the diagonal nature of  $\mathbf{H}$ , the optimal  $\mathbf{Q}$  is also diagonal. In particular, the uniform power allocation  $\mathbf{Q} = \frac{TP}{N_c D} \mathbf{I}_{N_c D} = \text{SNR } \mathbf{I}_{N_c D}$  achieves capacity and

$$C_{coh}(\text{SNR}) = \frac{\sum_{i=1}^D \mathbf{E} \left[ \log_2 \left( 1 + \frac{TP}{N_c D} |h_i|^2 \right) \right]}{D} \stackrel{(a)}{=} \mathbf{E} \left[ \log_2 \left( 1 + \text{SNR} |h|^2 \right) \right] \quad (25)$$

where (a) follows since  $\{h_i\}$  are i.i.d. with  $h$  representing a generic random variable,  $N_c D = TW$  and  $\text{SNR} = \frac{P}{W}$ .

The next proposition provides upper and lower bounds to the coherent capacity in the low SNR regime.

*Proposition 1:* For all  $b \in (0, 1)$  and  $\text{SNR} = \frac{P}{W}$  such that  $\text{SNR} < \frac{(1-b)}{b}$ , the coherent capacity satisfies

$$C_{coh}(\text{SNR}) \geq \log_2(e) (\text{SNR} - \text{SNR}^2) \\ C_{coh}(\text{SNR}) \leq \log_2(e) \left( \text{SNR} - \frac{b}{2} \cdot \text{SNR}^2 \right). \quad (26)$$

Moreover the capacity converges to the lowerbound as  $\text{SNR} \rightarrow 0$ .

*Proof:* See Appendix A. ■

The lowerbound in Proposition 1 shows that the minimum energy per bit for reliable communication is given by  $\frac{E_b}{N_o \min} = \log_e(2)$  and the wideband slope  $S_0 = 1$ , the two fundamental metrics defined in [7].

We now define the notion of an *operational coherence level* [8] that allows an alternative, but equivalent, characterization of capacity in the wideband/low-SNR regime.

*Definition 1:* Let  $I_{tr}$  be the average mutual information achievable with a training-based communication scheme. We say that the scheme achieves an operational coherence level of  $\epsilon$  ( $0 \leq \epsilon \leq 1$ ) if the low SNR asymptote of  $I_{tr}$  is of the form  $\text{SNR} - \mathcal{O}(\text{SNR}^{1+\epsilon})$ . Note that the two values of  $\epsilon = 0$  and  $\epsilon = 1$  correspond to the first-order and second-order optimality conditions, respectively, as defined in [7]. ■

In the scaling law,  $N_c = \frac{1}{\text{SNR}^\mu}$ ,  $\mu > 0$  in (17), the parameter  $\mu$  reflects the coherence achieved by the training-based communication scheme. We are interested in computing the value of  $\mu$  such that the training-based scheme achieves an operational coherence level of  $\epsilon$ . This relation is characterized in Theorem 1. We start with the following lemma that provides a lower bound to the capacity of the training-based scheme.

*Lemma 1:* The capacity of the training-based communication scheme described in Sec. II-C is lower bounded by

$$I_{tr}(\eta, N_c, \text{SNR}) \geq \hat{I}_{tr}(\eta, N_c, \text{SNR}) \triangleq \frac{1}{2} \log_2 (1 + 2\beta\sigma^2) \quad (27)$$

where

$$\beta(\eta, N_c, \text{SNR}) = \frac{(1-\eta)(1+\eta)N_c\text{SNR}}{[(N_c-1)(1+\eta)N_c\text{SNR} + (1-\eta)N_c\text{SNR}]} \quad (28)$$

$$\sigma^2(\eta, N_c, \text{SNR}) = \frac{\eta N_c \text{SNR}}{1+\eta N_c \text{SNR}}. \quad (29)$$

*Proof:* See Appendix B. ■

Next, we optimize over the fraction of energy spent for training,  $\eta$ , to maximize the lower bound  $\hat{I}_{tr}$ . Thus, we explicitly highlight the role of  $\eta$  in the following lemma.

*Lemma 2:* The  $\eta$  that maximizes  $\hat{I}_{tr}(\eta)$  given in (27) satisfies  $\frac{dK(\eta)}{d\eta} = 0$  where  $K(\eta) = K = \beta\sigma^2$  and  $\beta$  and

$\sigma^2$  are as in (28) and (29), respectively. The optimizing value  $\eta^*$  and the corresponding  $K^*$  are given by

$$\eta^* = \frac{N_c \text{SNR} + N_c - 1}{(N_c - 2) N_c \text{SNR}} \cdot \left[ \sqrt{1 + \frac{N_c \text{SNR} (N_c - 2)}{N_c \text{SNR} + N_c - 1}} - 1 \right] \quad (30)$$

$$K^* = \frac{N_c \text{SNR} + N_c - 1}{(N_c - 2)^2} \cdot \left[ \sqrt{1 + \frac{N_c \text{SNR} (N_c - 2)}{N_c \text{SNR} + N_c - 1}} - 1 \right]^2. \quad (31)$$

Furthermore, the optimized (tightest) lower bound is given by

$$\hat{I}_{tr}(\eta^*) = \left( 1 - \frac{1}{N_c} \right) \cdot \frac{1}{2} \cdot \log_2 (1 + 2K^*). \quad (32)$$

*Proof:* See Appendix C. ■

We now state the main result of this work. The following theorem characterizes the required scaling of  $N_c$  (value of  $\mu$ ) so that any operational coherence level  $\epsilon$  can be achieved.

*Theorem 1:* The average mutual information of the training-based scheme achieves an operational coherence level  $\epsilon \in [0, 1]$

$$I_{tr} \geq \log_2(e) \cdot [\text{SNR} - \mathcal{O}(\text{SNR}^{1+\epsilon})] \quad (33)$$

if and only if  $N_c = \frac{1}{\text{SNR}^\mu}$  for  $\mu > 1 + 2\epsilon$ . More precisely, if  $\epsilon \in [0, 1)$  and  $N_c = \frac{1}{\text{SNR}^\mu}$ ,  $\mu > 1 + 2\epsilon = 1$ , then

$$I_{tr} \geq \log_2(e) \cdot [\text{SNR} - 2 \text{SNR}^{1+\epsilon} + o(\text{SNR}^{1+\epsilon})]. \quad (34)$$

If  $\epsilon = 1$  and  $N_c = \frac{1}{\text{SNR}^3}$ , then

$$I_{tr} \geq \log_2(e) \cdot [\text{SNR} - 3 \text{SNR}^2 + o(\text{SNR}^2)]. \quad (35)$$

If  $\epsilon = 1$  and  $N_c = \frac{1}{\text{SNR}^\mu}$ ,  $\mu > 1 + 2\epsilon = 3$ , then

$$I_{tr} \geq \log_2(e) \cdot [\text{SNR} - \text{SNR}^2 + o(\text{SNR}^2)]. \quad (36)$$

In particular, the first- and second-order optimality conditions (corresponding to  $\epsilon = 0$  and  $\epsilon = 1$ ) are met if and only if  $\mu > 1$  and  $\mu > 3$ , respectively.

*Proof:* See Appendix D. ■

Theorem 1 and equation (18) are key to understanding the impact of sparsity on achieving coherent capacity in the UWB regime. This is discussed in the next section.

## IV. DISCUSSION OF RESULTS

### A. The Coherence Dimension: Sharing Coherence Costs in Time and Frequency

Multipath sparsity provides a natural mechanism for channel coherence and our results underscore the impact of sparsity in both delay and Doppler via the notion of the time-frequency coherence dimension,  $N_c$ . As discussed in Section II-A, in sparse channels,  $D_W$  and  $W_{coh}$  increase sub-linearly with  $W$ . Furthermore, unlike existing works, we explicitly account for Doppler diversity –  $D_T$  and  $T_{coh}$  increase sub-linearly with  $T$  – since STF signaling involves coding over multiple coherence times.

Theorem 1 shows that the requirement on  $T_{coh}$  in [8] is now the requirement on time-frequency coherence dimension  $N_c = T_{coh} W_{coh}$ . Thus, the coherence cost is shared in both time and frequency and as a result the required scaling for  $T_{coh}$  can be *significantly weakened* by taking advantage of the natural scaling of  $W_{coh}$  with  $W$ . If the delay diversity is

known to scale as  $D_W = \mathcal{O}(W^{\delta_2}) \leftrightarrow W_{coh} = \mathcal{O}(W^{1-\delta_2})$ , then the  $T_{coh}$  scaling requirement reduces to

$$T_{coh} = N_c / W_{coh} = \mathcal{O}(W^{2\epsilon + \delta_2}) \quad (37)$$

to achieve an operational coherence level  $\epsilon$ , as per Definition 1. For example, using  $\epsilon = 0.5$ , which corresponds to a sub-linear term of  $\text{SNR}^{1.5}$  in (33), and  $\delta_2 = 0.5$ , we get  $T_{coh} = \mathcal{O}(W^{1.5})$ . This is a less stringent scaling law than would be required using the framework of [8], where the requirement would be  $T_{coh} = \mathcal{O}(W^{1+2\epsilon}) = \mathcal{O}(W^2)$ . The weaker  $T_{coh}$  requirement for sparse channels is graphically illustrated in Fig. 2(a) for the following parameters:  $T_m = 10^{-5}$  secs.,  $W_d = 50$  Hz,  $W = 50$  MHz. Note that as the channel becomes more sparse in delay (decreasing  $\delta_2$ ),  $W_{coh}$  gets larger, thereby reducing the  $T_{coh}$  requirement to achieve any desired operational coherence  $\epsilon$ .

### B. Asymptotic Coherence of Sparse Channels

Since channel uncertainty is the main factor that affects capacity in the non-coherent scenario, we further investigate the performance of channel estimation using two metrics: (i) MSE of channel estimates and (ii) optimal fraction of total energy used for estimation,  $\eta^*$ . The following theorem characterizes the value of  $\mu$  for asymptotically energy-efficient and consistent estimation.

*Theorem 2:* In the limit of large signal space dimension ( $T, W \rightarrow \infty$ )

$$\eta^* \rightarrow 0 \quad \text{and} \quad \text{MSE} = \frac{1}{1 + E_{tr}} \rightarrow 0 \quad (38)$$

if and only if  $N_c = \frac{1}{\text{SNR}^\mu}$  and  $\mu > 1$ .

Furthermore, the rates of convergence are given by

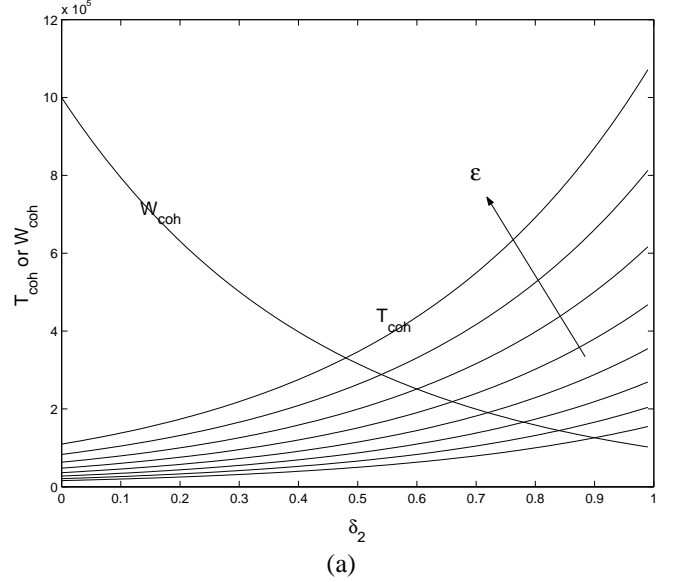
$$\eta^* \rightarrow 0 \quad \text{as} \quad \mathcal{O}\left(\frac{1}{\sqrt{N_c \text{SNR}}}\right) = \mathcal{O}\left(\text{SNR}^{\frac{\mu-1}{2}}\right) = \mathcal{O}\left(W^{\frac{1-\mu}{2}}\right)$$

$$E_{tr} \rightarrow \infty \quad \text{as} \quad \mathcal{O}\left(\sqrt{N_c \text{SNR}}\right) = \mathcal{O}\left(\text{SNR}^{\frac{1-\mu}{2}}\right) = \mathcal{O}\left(W^{\frac{\mu-1}{2}}\right). \quad (39)$$

*Proof:* See Appendix E. ■

The above result says that multipath wireless channels are *asymptotically coherent* if and only if they are sparse and  $N_c$  satisfies the condition ( $\mu > 1$ ) specified in Theorem 2. For rich multipath,  $N_c$  is a constant ( $N_c = \frac{1}{T_m W_d}$ ) and does not scale with SNR. For a sparse channel with  $\mu \leq 1$ ,  $N_c$  does not scale at a fast enough rate with SNR. Under both scenarios, as shown in the proof of the theorem, the training scheme asymptotically uses half the total energy ( $\eta^* \rightarrow 0.5$ ) to estimate the channel coefficients and the MSE does not decay to zero. For  $\mu = 1$ , the estimation performance is better than when  $\mu < 1$ , but still not good enough to obtain asymptotic coherence. These observations are illustrated in Fig. 2(b) where  $\eta^*$  and MSE are plotted as a function of increasing bandwidth for three different cases:  $\mu = 0.7$ ,  $\mu = 1$  and  $\mu = 1.3$ . In all the three cases, the signaling duration  $T$  is chosen according to (18).

Note that the requirement ( $\mu > 1$ ) for asymptotic coherence in Theorem 2 is exactly the same as the condition to achieve first-order optimality in Theorem 1. This makes intuitive sense:



(a)  $\delta = 0.5, T_m = 1 \mu\text{s}, W_d = 100 \text{ Hz}$

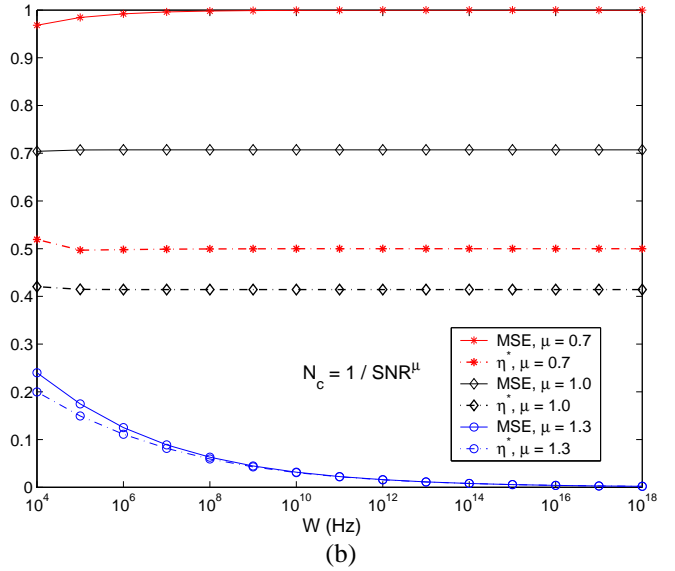


Fig. 2. (a) The variation of  $T_{coh}$  and  $W_{coh}$  as a function of delay sparsity ( $\delta_2$ ). (b) MSE and  $\eta^*$  for the channel estimation scheme as a function of  $W$  for three different values of  $\mu$ .

with diminishing channel uncertainty ( $\text{MSE} \rightarrow 0$ ) and a vanishing fraction of the energy ( $\eta^* \rightarrow 0$ ) used for estimation, the capacity of the training-based system converges to coherent capacity in the wideband limit.

### C. Optimal Choice of Signaling Parameters

Recall the discussion in Section II-B, in particular equation (18) that relates the signaling parameters ( $T, W, P$ ) for achieving a desired scaling of  $N_c$  with SNR in (17). We now revisit this relationship, in light of Theorem 1, and investigate the choice of signaling parameters in order to obtain a desired level of operational coherence  $\epsilon$  (in particular, the values for first- and second-order optimality,  $\epsilon = 0$  and  $\epsilon = 1$ , respectively).

Theorem 1 states that to achieve an operational coherence

$\epsilon$ , the coherence dimension must scale as

$$N_c = \frac{1}{\text{SNR}^\mu}, \quad \mu > 1 + 2\epsilon \quad (40)$$

and by taking the logarithm of (18) we note that the signaling duration  $T$  must scale with  $W$  as a function of  $P$  and the channel sparsity parameters as

$$\log(T) = \frac{1}{1-\delta_1} \log(W_d^{\delta_1} T_m^{\delta_2}) + \left(\frac{\mu + \delta_2 - 1}{1-\delta_1}\right) \log(W) - \left(\frac{\mu}{1-\delta_1}\right) \log(P). \quad (41)$$

For example, with  $T_m W_d = 10^{-6}$ ,  $\frac{P}{N_0} = 30$  dB,  $W = 1$  GHz and a sparsity of  $\delta_1 = \delta_2 = 0.5$ , the required minimum signaling duration to obtain first-order optimality ( $\epsilon = 0$ ,  $\mu > 1$ ) is  $T \approx 1$  ms.

Note from (41) that smaller  $\delta_i$ 's imply a slower scaling of  $T$  with  $W$ . Conversely, for a given  $T$  and  $W$ , (41) can be used to determine the effective value of  $\mu$  in (40) as

$$\mu_{\text{eff}} = \frac{(1-\delta_1) \log(T/c) + (1-\delta_2) \log(P)}{\log(W/P)} + (1-\delta_2) \quad (42)$$

where  $c = \left(T_m^{\delta_2} W_d^{\delta_1}\right)^{\frac{1}{1-\delta_1}}$ . The effective operational coherence level can then be determined as  $\epsilon_{\text{eff}} = \frac{\mu_{\text{eff}} - 1}{2}$ .

Note that  $\mu_{\text{eff}} \rightarrow \infty$  as  $T \rightarrow \infty$  for sparse channels, which implies that any operational level of coherence can be achieved by simply increasing  $T$ . This is due to multipath sparsity in Doppler. This is illustrated in Fig. 3, where we consider the low SNR asymptote of the coherent capacity in (26). The coefficients of the first- and second-order terms are  $\lambda_1 = \log_2(e)$  and  $\lambda_2 = -\log_2(e)$ , respectively. In Fig. 3, we plot the numerically estimated values  $c_1$  and  $c_2$  of  $\lambda_1$  and  $\lambda_2$ , respectively, for the training-based scheme, which are estimated using Monte-Carlo simulations and using the optimized lower bound on  $I_{tr}$  in (32). For a large enough  $T$  such that  $\mu_{\text{eff}} > 1$ , the first-order constant  $c_1 \rightarrow \lambda_1 = \log_2(e)$ . Also shown in the figure is the behavior of the second-order constant and for an even larger value of  $T$ , we obtain  $c_2 \rightarrow \lambda_2 = -\log_2(e)$ , when  $\mu_{\text{eff}} > 3$ .

#### D. Peaky versus Non-Peaky Signaling

Several works have emphasized the necessity of signaling schemes that are peaky in time and/or frequency for achieving wideband capacity in the non-coherent regime [12], [16], [7]. The motivation behind peaky signaling is that communication takes place over a smaller set of signaling dimensions, thereby reducing the effect of channel uncertainty since fewer channel parameters need to be estimated. However, peaky signaling is practically infeasible due to peak power constraints. More importantly, the requirement of peakiness in these works is tied with the implicit assumption of rich multipath.

When the channel is sparse, the coherence dimension  $N_c$  naturally scales with the signal space dimension ( $N = TW$ ) and this new effect raises the following question: Is peaky signaling still necessary to achieve capacity in the wideband limit? Theorem 1 provides the answer: as long as  $\mu > 1$ , non-peaky i.i.d. Gaussian input signals are first-order optimal and

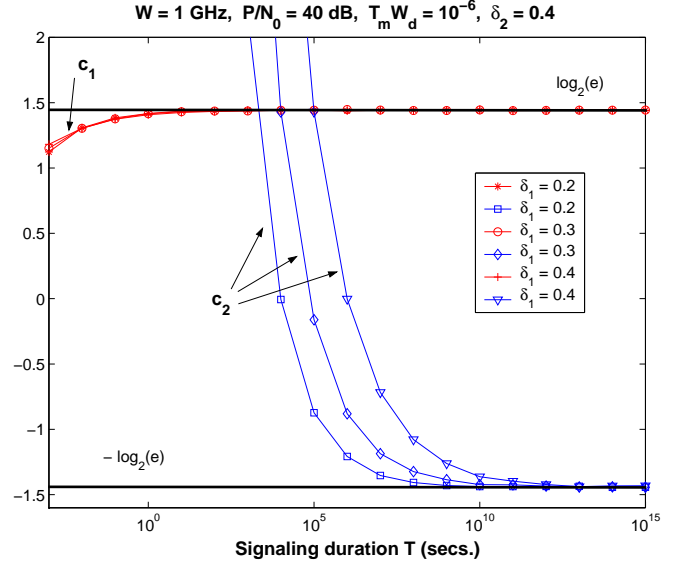


Fig. 3. Numerically estimated values of capacity metrics. Convergence of the coefficients of the SNR and SNR<sup>2</sup> terms in capacity as a function of  $T$ .

with  $\mu > 3$ , second-order optimality is also satisfied. While the authors in [8, Lemma 2] (using a non-peaky training-based communication scheme) obtained exactly the same conditions on  $\mu$ , their results are for the scaling of  $T_{coh}$ , whereas our scaling result in Theorem 1 is for  $N_c = T_{coh} W_{coh}$ . In order to weaken the  $T_{coh}$  requirement, the authors in [8, Lemma 3] advocate the use of peaky training and communication. Furthermore, the capacity-optimal scheme according to [8, Theorem 4] is a peaky non-coherent communication scheme in which no explicit training is performed. Next, we present a detailed discussion on the scaling laws of  $T$  as a function of  $W$  to achieve a desired level of operational coherence. To illustrate the impact of sparsity, we compare the scaling requirements in this paper with those in [8].

From (41), we note that to achieve an operational coherence level of  $\epsilon$ ,  $T$  must scale with  $W$  as

$$T_{\text{sparse}} \propto W^{\frac{2\epsilon + \delta_2}{1-\delta_1}} \quad (43)$$

where the subscript on  $T$  emphasizes that it applies to sparse channels. On the other hand, the corresponding scaling on  $T$  for either the peaky or the non-peaky training-based communication scheme in [8, Lemma 2 and 3], can be inferred as

$$T_{\text{rich}} \propto \text{SNR}^{-(1+2\epsilon)} \propto W^{1+2\epsilon} \quad (44)$$

This is because when there is no peakiness, then the minimum signaling duration is  $T = T_{coh} \propto \text{SNR}^{-(1+2\epsilon)}$ . When peaky training and communication is used,  $T = L \cdot T_{coh} \propto [\text{SNR}^{\epsilon-1}] \cdot [\text{SNR}^{-3\epsilon}] = \text{SNR}^{-(1+2\epsilon)}$ .

Thus, (43) yields a slower (less stringent) scaling than (44) when

$$\frac{2\epsilon + \delta_2}{1-\delta_1} < 1 + 2\epsilon \iff (1+2\epsilon)\delta_1 + \delta_2 < 1. \quad (45)$$

The locus of points in the  $(\delta_1, \delta_2)$  plane represented in (45) defines the set of channel sparsity values for which we obtain a slower scaling requirement. This is pictorially represented in

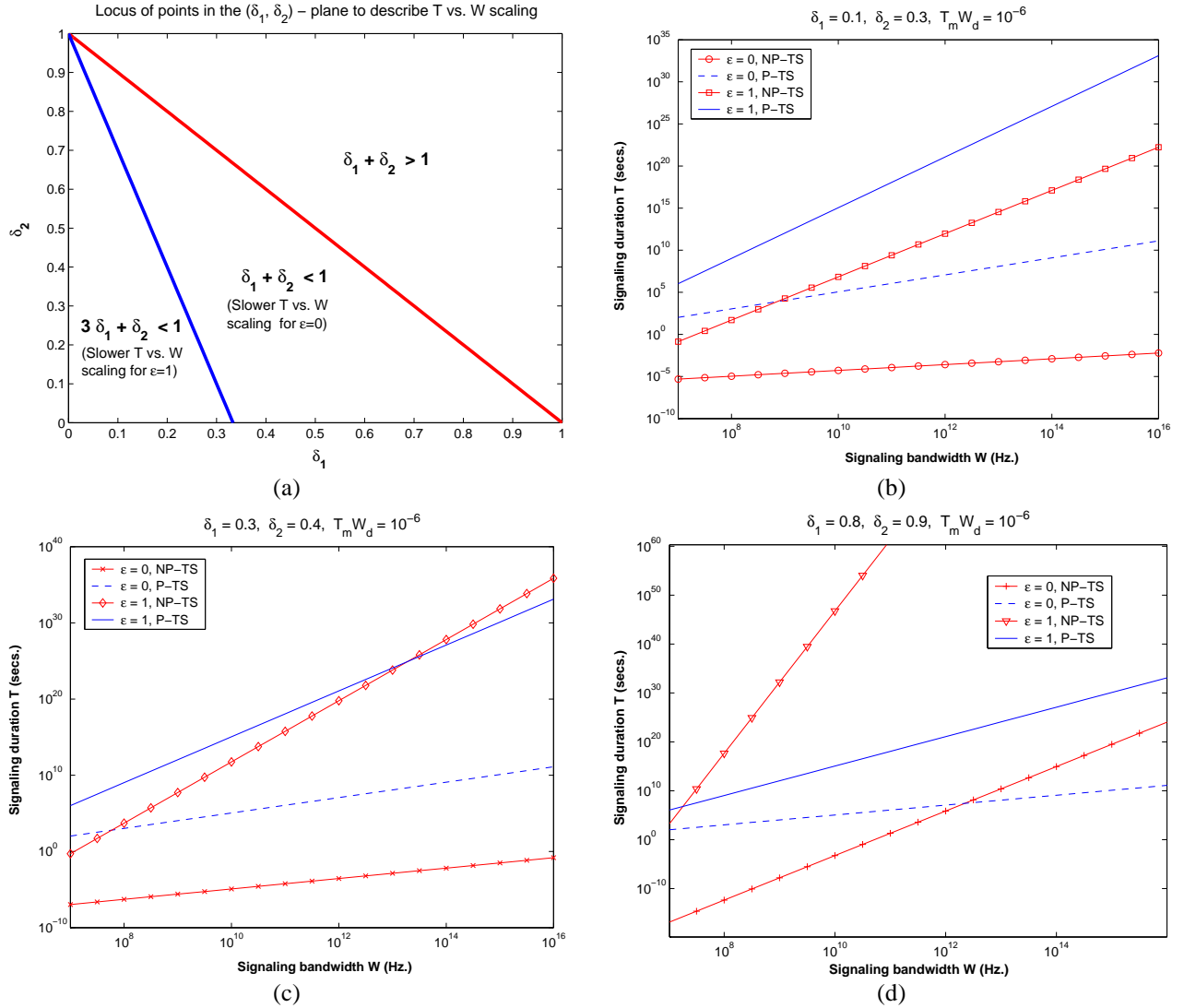


Fig. 4. (a) Regions in the  $(\delta_1, \delta_2)$  plane comparing the required  $T$  vs.  $W$  scaling in the NP-TS and P-TS schemes. Points to the left of the  $\delta_1 + \delta_2 = 1$  line represent the favorable region for first-order optimality ( $\epsilon = 0$ ) of NP-TS, illustrated in (c); for points to the right of this line, P-TS yields more favorable scaling, illustrated in (d). Points to the left of the  $3\delta_1 + \delta_2 < 1$  line represent the favorable region for second-order optimality ( $\epsilon = 1$ ) of NP-TS, illustrated in (b). (b)-(d):  $T$  vs.  $W$  scaling comparison for the two schemes for different levels of sparsity. (b) High sparsity:  $\delta_1 = 0.1$  and  $\delta_2 = 0.3$ . (c) Medium sparsity:  $\delta_1 = 0.3$  and  $\delta_2 = 0.4$ . (d) Low sparsity:  $\delta_1 = 0.8$  and  $\delta_2 = 0.9$ .

Fig. 4(a) for the special cases of  $\epsilon = 0$  (first-order optimality) and  $\epsilon = 1$  (second-order optimality).

Figs. 4(b)-(d) illustrate the required scaling of  $T$  with  $W$  for different levels of channel sparsity. In all figures, the non-peaky training-based scheme in our framework is denoted by NP-TS, whereas the peaky training scheme in [8] is denoted by P-TS. The signaling duration requirements for P-TS are independent of channel sparsity and are given by

$$T_{p-ts,1} \propto W, \quad T_{p-ts,2} \propto W^3 \quad (46)$$

where the subscripts “1” and “2” reflect the requirements for first- and second-order optimality, respectively. Fig. 4(b) compares the scaling requirements for the sparsest channel:  $\delta_1 = 0.1$  and  $\delta_2 = 0.3$  so that  $3\delta_1 + \delta_2 < 1$ . In this case, the scaling requirements for NP-TS are:

$$T_{np-ts,1} \propto W^{1/3} < W, \quad T_{np-ts,2} \propto W^{2.3/0.9} < W^3 \quad (47)$$

which are less stringent than (46) for both first- and second-

order optimality. Fig. 4(b) corresponds to a medium sparse channel:  $\delta_1 = 0.3$  and  $\delta_2 = 0.4$ . In this case, the scaling requirements for NP-TS are

$$T_{np-ts,1} \propto W^{0.4/0.7} < W, \quad T_{np-ts,2} \propto W^{2.4/0.7} > W^3 \quad (48)$$

which are less stringent than (46) for first-order optimality but more stringent for second-order optimality. Fig. 4(c) represents the least sparse channel:  $\delta_1 = 0.8$  and  $\delta_2 = 0.9$  so that  $\delta_1 + \delta_2 > 1$ . In this case, the scaling requirements for NP-TS are

$$T_{np-ts,1} \propto W^{0.9/0.2} > W, \quad T_{np-ts,2} \propto W^{2.9/0.2} > W^3 \quad (49)$$

which are more stringent than (46) for both first- and second-order optimality.

#### E. Rich versus Sparse Multipath: The Extreme Cases

We now discuss the two extreme scenarios of rich and sparse multipath, i.e.  $\delta_i \rightarrow 0$  or  $1$ ,  $i = 1, 2$ . The canonical scaling

relationship in (18) between  $T$  and  $W$  (ignoring constants) is

$$T \propto W^{\frac{\mu+\delta_2-1}{1-\delta_1}}. \quad (50)$$

As either  $\delta_1$  or  $\delta_2$  or both tend to zero, we have a very sparse channel in which any desired value of  $\mu$  can be obtained with relatively small values of  $T$  by following (50).

When  $\delta_2 \rightarrow 1$ , the conditions on  $T$  in (50) grow more stringent in order to attain a desired  $\mu$ . When  $\delta_2 = 1$ ,  $W_{coh}$  is a constant and the requirements on  $N_c$  can be attained only through  $T_{coh}$  scaling with increasing  $T$ . In particular, the conditions on  $T$  in (50) become

$$T \propto W^{\frac{\mu}{1-\delta_1}}. \quad (51)$$

As  $\delta_1 \rightarrow 1$ , the conditions on  $T$  to attain a desired  $\mu$  become more stringent. When  $\delta_1 = 1$ , we have a constant  $T_{coh}$  and from a scaling perspective,  $N_c = W_{coh} \propto W^{1-\delta_2} = \frac{1}{\text{SNR}^{1-\delta_2}}$ . Thus the attained value of  $\mu$  is  $\mu = 1 - \delta_2 \leq 1$ , and even first-order optimality cannot be obtained.

This issue can be resolved by considering peaky signaling schemes, that also help offset the large  $T$  requirements when  $\delta_1$  and/or  $\delta_2$  is close to 1. We model peaky signaling by assuming that a subset of the time-frequency coherence subspaces in each codeword (Fig. 1(b)) are used for training and communication and no information is sent in the remaining subspaces. We model peakiness similar to [8] and define

$$\zeta = \text{SNR}^\gamma, \quad \gamma > 0 \quad (52)$$

as the fraction of signal space dimensions which are used for communication. The effect of peakiness is captured through the parameter  $\gamma$ . More specifically, the peakiness ratio (PR) between peaky and non-peaky signaling given by  $\text{PR} = \frac{\text{SNR}'}{\text{SNR}} = \text{SNR}^{-\gamma} \rightarrow \infty$  as  $\text{SNR} \rightarrow 0$  since  $\gamma > 0$ . It is clear that  $\gamma < 1$ , since the energy per transmit symbol equals

$$\text{SNR}' = \frac{\text{SNR}}{\text{SNR}^\gamma} = \text{SNR}^{1-\gamma} \quad (53)$$

and  $\text{SNR}' \geq 1$  when  $\gamma \geq 1$  and we are no longer in the low SNR regime. The following result captures the impact of peakiness on the average mutual information of the training-based scheme.

*Proposition 2:* The peaky training-based scheme achieves

$$I_{tr}^p(\text{SNR}) \geq \log_2(e) \cdot \left[ \text{SNR} - \mathcal{O}\left(\text{SNR}^{\frac{1+\mu}{2}}\right) \right] \quad (54)$$

if  $N_c = 1/\text{SNR}^{\mu-\gamma}$ .

*Proof:* The average mutual information with a peaky input equals

$$I_{tr}^p(\text{SNR}) = \zeta I_{tr}(\text{SNR}') = \text{SNR}^\gamma I_{tr}(\text{SNR}') \quad (55)$$

where  $I_{tr}(\text{SNR}')$  is the average mutual information achievable with the non-peaky scheme, as in (33) of Theorem 1. Therefore, if

$$N_c = \frac{1}{\text{SNR}^{\mu-\gamma}} = \frac{1}{(\text{SNR}')^{\frac{\mu-\gamma}{1-\gamma}}}$$

then, using (55) and (33), we have

$$\begin{aligned} I_{tr}^p(\text{SNR}) &\geq \log_2(e) \cdot \text{SNR}^\gamma \cdot \left[ \text{SNR}' - \mathcal{O}\left(\left(\text{SNR}'\right)^{\frac{1+\frac{\mu-\gamma}{2}}{1-\gamma}}\right) \right] \\ &\stackrel{(a)}{=} \log_2(e) \cdot \text{SNR}^\gamma \cdot \left[ \text{SNR}^{1-\gamma} - \mathcal{O}\left(\text{SNR}^{\frac{1+\mu-2\gamma}{2}}\right) \right] \\ &= \log_2(e) \cdot \left[ \text{SNR} - \mathcal{O}\left(\text{SNR}^{\frac{1+\mu}{2}}\right) \right] \end{aligned} \quad (56)$$

where (a) follows from (53). This proves the proposition. ■ Thus the advantage of using a peaky input manifests itself in reducing the required SNR exponent of the coherence dimension,  $N_c$ . That is, the effective  $\mu$  reduces to  $\mu_{\text{peaky}} = \mu - \gamma$ . Using the result of Proposition 2, we now revisit the scaling law in (18). As a consequence of the condition  $N_c = 1/\text{SNR}^{\mu-\gamma}$ , we obtain a slower (relaxed) scaling of  $T$  as a function of  $W$  to achieve a desired value of  $\mu$

$$T \propto W^{\frac{\mu+\delta_2-1-\gamma}{1-\delta_1}}. \quad (57)$$

For any  $0 < \delta_1, \delta_2 < 1$ , the rate at which  $T$  scales with  $W$  can now be controlled through the peakiness parameter  $\gamma$ , especially when  $\delta_i \rightarrow 1$ . More importantly, when  $\delta_1 = 1$ , we have  $N_c = W_{coh} = \frac{1}{\text{SNR}^{1-\delta_2}}$  and therefore we can satisfy the condition  $N_c = 1/\text{SNR}^{\mu-\gamma}$  as long as

$$\gamma \geq \mu + \delta_2 - 1. \quad (58)$$

Note that while we can obtain first-order optimality in this case, and necessarily through peaky signaling, second-order optimality is not feasible since it requires  $\gamma \geq (2 + \delta_2) > 1$ . When  $\delta_2 = 1$ , peakiness is not necessary, but the scaling requirements on  $T$  can be relaxed from (51) to

$$T \propto W^{\frac{\mu-\gamma}{1-\delta_1}}. \quad (59)$$

## F. Arbitrary Sub-linear Scaling Laws

We modeled sparsity in delay and Doppler by restricting our attention to the power-law scaling in (7). We now show that the results in this paper hold true for *any* sub-linear scaling in the DoF. Since sparsity in delay/Doppler implies that  $W_{coh}$  and  $T_{coh}$  scale (sub-linearly) with  $W$  and  $T$  respectively, we assume a general scaling law for these quantities. Let

$$W_{coh} = f_1(W), \quad T_{coh} = f_2(T) \quad (60)$$

$$\implies N_c = T_{coh}W_{coh} = f_1(W)f_2(T) \quad (61)$$

where  $f_1$  and  $f_2$  are strictly increasing, arbitrary sub-linear functions of  $W$  and  $T$  respectively. That is,  $f_1(W) \sim o(W)$  and  $f_2(T) \sim o(T)$ . Note that the definition in (60) implies that  $D_W = \frac{W}{f_1(W)} \sim o(W)$  and  $D_T = \frac{T}{f_2(T)} = o(T)$ . We also assume

$$T = f_3(W) \quad (62)$$

where  $f_3$  reflects the scaling of  $T$  with  $W$ , necessary to obtain a desired value of  $\mu$ . Given  $f_1$  and  $f_2$ , our focus here is to find a suitable  $f_3$  so that a desired value of  $\mu$  can be obtained.

A key observation from Theorem 1 is that it provides necessary and sufficient conditions for first- and second-order

optimality that are *independent* of the power-law scaling assumptions in (7). Recall that with  $N_c = \frac{1}{\text{SNR}^\mu}$ , the condition for first-order optimality is  $\mu > 1$  and that for second-order optimality is  $\mu > 3$ . Defining a new parameter  $E_d = N_c \text{SNR} = \text{SNR}^{1-\mu}$ , which has the physical interpretation of the transmit energy per DoF, we have in the limit of  $\text{SNR} \rightarrow 0$ ,  $E_d \rightarrow \infty$  as  $\mathcal{O}\left(\frac{1}{\text{SNR}^{\mu-1}}\right)$  with  $\mu > 1$  and  $\mu > 3$  for first- and second-order optimality, respectively. Using (14) and (62), we have

$$\begin{aligned} E_d = N_c \text{SNR} &= f_1(W) f_2(T) \text{SNR} \\ &= f_1(W) f_2(f_3(W)) \text{SNR} \\ &= f_1(W) g_1(W) \text{SNR} \end{aligned} \quad (63)$$

where we have defined  $g_1(x) = (f_2 \circ f_3)(x)$ . We also provide the following definition that is used in the subsequent theorem.

*Definition 2:* For any two functions  $f$  and  $g$ , we define

$$f(x) \sim w(g(x)) \iff \lim_{x \rightarrow \infty} \left| \frac{f(x)}{g(x)} \right| = \infty. \quad (64)$$

*Theorem 3:* For the coherence scaling laws in (60) and (61), a necessary and sufficient condition to obtain a desired value of  $\mu$  is given by  $f_1(x) g_1(x) \sim w(x^\mu)$ .

*Proof:* Using (63) and noting that  $\text{SNR} = \frac{P}{W}$ , we have

$$N_c \text{SNR} = f_1\left(\frac{1}{\text{SNR}}\right) g_1\left(\frac{1}{\text{SNR}}\right) \text{SNR} = \frac{f_1(x) g_1(x)}{x}.$$

Therefore, to obtain a specific  $\mu$ , we require

$$\begin{aligned} N_c \text{SNR} = \mathcal{O}\left(\frac{1}{\text{SNR}^{\mu-1}}\right) &\iff \frac{f_1(x) g_1(x)}{x} = \mathcal{O}(x^{\mu-1}) \\ &\iff f_1(x) g_1(x) \sim w(x^\mu). \end{aligned} \quad (65)$$

Note that the conditions for first- and second-order optimality are  $f_1(x) g_1(x) \sim w(x)$  and  $f_1(x) g_1(x) \sim w(x^3)$ , respectively.

*Corollary 1:* For given  $f_1$  and  $f_2$ , the conditions of Theorem 3 are satisfied by choosing  $f_3(x) = f_2^{-1}\left(\frac{x^\mu}{f_1(x)}\right)$ .

*Remark 3:* The conditions of Theorem 3 are satisfied under the power-law scaling assumptions in (14) and the  $T$  vs.  $W$  scaling relationship in (18). We have  $f_1(x) = x^{1-\delta_2}$ ,  $f_2(x) = x^{1-\delta_1}$ ,  $f_3(x) = x^{\frac{\mu-1+\delta_2}{1-\delta_1}}$  and it follows that  $f_1(x) g_1(x) = x^\mu$ .

### G. Comments on Channel Modeling

A couple of comments on the channel model used in this paper are warranted. First, the block fading channel model in the STF domain used in this paper is an idealization of the effects of multipath sparsity in delay-Doppler. The idealized model was used to facilitate capacity analysis by relating the sub-linear scaling in the channel DoF in delay-Doppler to the scaling in the time-frequency coherence dimension under STF signaling. While the actual channel in the STF domain would exhibit more complex characteristics, the block fading idealization does capture the essence of multipath sparsity from the viewpoint of DoF scaling, which is the most

important channel property in the context of channel capacity in the limit of large signal space dimension.

Second, throughout this work, we assume a simplistic Gaussian model for small-scale fading. However, evidence from measurement campaigns suggests “specular” statistics for the channel coefficients and some channel measurements [1], [13] indicate that Nakagami or log-normal distributions may be a more accurate fit for the small-scale fading in the wideband regime. While this issue is not addressed in this paper, our assumption of Gaussian statistics permits closed-form analysis and we suspect that the implications of multipath sparsity would hold under such statistics as well.

## V. CONCLUSIONS

We have investigated the ergodic capacity of sparse multipath channels in the ultrawideband regime. Motivated by recent measurement campaigns, we have introduced a model for sparse multipath channels that captures the effect of multipath sparsity on the statistically independent DoF in the channel via the notion of resolvable paths in delay and Doppler. The workhorse of our analysis is the use of orthogonal STF signaling that approximately diagonalizes underspread channels and naturally relates multipath sparsity in delay-Doppler to coherence in time and frequency. In particular, we proposed a simple block-fading model for sparse channels in the STF domain that captures the sub-linear scaling of the channel DoF with signal space dimensions.

Our work builds on recent results on ergodic capacity in the wideband regime to study the impact of multipath sparsity on bridging the gap between coherent and non-coherent regimes. The most significant implication of multipath sparsity is that the requirements on coherence time,  $T_{coh}$ , in existing works [8] are naturally replaced by requirements on the time-frequency coherence dimension,  $N_c = T_{coh} W_{coh}$ . As a result the requirements on channel coherence are shared between time and frequency thereby leading to significantly reduced coherence time requirements to attain a desired level of coherence. Our results reveal how any desired operational coherence can be achieved by scaling the signaling parameters – signaling duration  $T$ , bandwidth  $W$  and transmit power  $P$  – in an appropriate fashion. We also discussed the usefulness of peaky signaling schemes for reducing coherence requirements and the role played by channel sparsity in relaxing peakiness requirements.

There are many interesting directions for future work. First, it would be useful to refine the results in this paper via more accurate modeling of sparsity in the time-frequency domain (as opposed to the block fading model). Second, studying the impact of non-Gaussian statistics of channel coefficients would also be useful. Third, while ergodic capacity is achieved by coding over long signaling durations, in practical settings with strict delay constraints, it is important to investigate more relevant metrics, like outage capacity [17]. An important and related performance metric is reliability (in terms of error exponents) [18]. We are currently investigating the impact of multipath sparsity on outage capacity and reliability. In this context, we recently reported a new fundamental *learnability*

versus diversity tradeoff in sparse channels that governs the impact of sparsity on reliability and error probability [19]. Another interesting aspect to study is the impact of feedback on achievable rates [20],[21]. Finally, we note that sparse channel models arise in other scenarios as well, such as underwater acoustic channels (see e.g., [22]). Thus the implications of this work may be applicable in such situations as well.

## APPENDIX

### A. Proof of Proposition 1

As is well known, the coherent capacity expression can be computed in closed-form using standard integral formulas. For this, we use the following fact [23, 4.337(1), pp. 574]:

$$\int_0^\infty \log_e(a+x)e^{-bx} dx = \frac{1}{b} \left[ \log_e(a) + e^{ab} \int_{ab}^\infty \frac{e^{-t}}{t} dt \right]. \quad (66)$$

Particularizing (66) to  $\mathbf{E} \left[ \log_2 \left( 1 + \text{SNR} |h|^2 \right) \right]$  by a transformation of random variables of the form  $\text{Re}(h) = r \cos(\theta)$ ,  $\text{Im}(h) = r \sin(\theta)$  results in

$$C_{coh}(\text{SNR}) = e^{\frac{1}{\text{SNR}}} \int_{\frac{1}{\text{SNR}}}^\infty \frac{e^{-t}}{t} dt. \quad (67)$$

We can then bound  $C_{coh}(\text{SNR})$  using [24, 5.1.20, pp.229] as

$$\frac{1}{2} \log_e(1+2\text{SNR}) \leq e^{\frac{1}{\text{SNR}}} \int_{\frac{1}{\text{SNR}}}^\infty \frac{e^{-t}}{t} dt \leq \log_e(1+\text{SNR}). \quad (68)$$

The upper bound of the proposition follows from a combination of Jensen's inequality and the monotonicity of  $\log_e(1+x) - x + \frac{bx^2}{2}$  under the imposed constraints on  $b$ . The lower bound follows via a Taylor's series truncation. The tightness of the lower bound at low SNR follows from the asymptotic (in  $\frac{1}{\text{SNR}}$ ) expansion of the exponential integral [24, 5.1.51, pp. 231]. ■

### B. Proof of Lemma 1

We begin with the vectorized system equation for the communication component of the scheme (described in (22))

$$\mathbf{y} = \mathbf{H}\mathbf{x} + \mathbf{w} = \widehat{\mathbf{H}}\mathbf{x} + \Delta\mathbf{x} + \mathbf{w}. \quad (69)$$

Here, we have represented the  $(N_c-1)D$ -dimensional communication sub-channel of the diagonal channel in (10) by  $\widehat{\mathbf{H}}$  for simplicity.  $\widehat{\mathbf{H}}$  is the  $(N_c-1)D$ -dimensional diagonal matrix of channel estimates and  $\Delta$  is the estimation error matrix,  $\Delta = \mathbf{H} - \widehat{\mathbf{H}}$ . Lumping the estimation error along with the additive noise and optimizing over the set of input covariance matrices  $\mathbf{Q}$  that satisfy  $\text{Tr}(\mathbf{Q}) = (1-\eta)TP$ , a lower bound to  $I_{tr}$  is achieved [25] as follows:

$$I_{tr} \geq \sup_{\mathbf{Q}} \frac{\mathbf{E} \left[ \log_2 \det \left( \mathbf{I} + \widehat{\mathbf{H}}\mathbf{Q}\widehat{\mathbf{H}}^H (\mathbf{I} + \Sigma_{\Delta\mathbf{x}})^{-1} \right) \right]}{N_c D} \quad (70)$$

where  $\mathbf{I}$  denotes the  $(N_c-1)D$  dimensional identity matrix. We use a zero-mean Gaussian input with covariance matrix  $\mathbf{Q} = \frac{\text{Tr}(\mathbf{Q})}{(N_c-1)D} \mathbf{I}$ . With this choice, note that  $\Sigma_{\Delta\mathbf{x}} =$

$\mathbf{E}_{\mathbf{H},\mathbf{x}} [\Delta\mathbf{x}\mathbf{x}^H \Delta^H] = \mathbf{E}_{\mathbf{H}} [\Delta\mathbf{Q}\Delta^H] = \frac{1}{1+E_{tr}} \cdot \frac{\text{Tr}(\mathbf{Q})}{(N_c-1)D} \mathbf{I}$  since  $h_i$  are identically distributed. Thus, we have

$$\begin{aligned} I_{tr} &\geq \frac{1}{N_c D} \cdot \mathbf{E} \left[ \log_2 \det \left( \mathbf{I} + \beta \widehat{\mathbf{H}}\widehat{\mathbf{H}}^H \right) \right] \\ &= \left( \frac{N_c-1}{N_c D} \right) \cdot \sum_{i=1}^D \mathbf{E} \left[ \log_2 \left( 1 + \beta |\widehat{h}_i|^2 \right) \right] \\ &\stackrel{(a)}{=} \left( 1 - \frac{1}{N_c} \right) \cdot \mathbf{E} \left[ \log_2 \left( 1 + \beta |\widehat{h}|^2 \right) \right] \end{aligned} \quad (71)$$

where  $\beta$  is as in (28) and (a) follows because the random variables  $\{\widehat{h}_i\}$  are i.i.d. Furthermore, it can be shown that the  $\widehat{h}_i$ 's are zero-mean with  $\mathbf{E}[|\widehat{h}_i|^2] = \mathbf{E}[|\widehat{h}|^2] = \sigma^2$  as in (29). We now compute the expectation in (71) in closed-form. For this, we use (66) [23, 4.337(1), pp. 574]. Particularizing (66) to  $\mathbf{E} \left[ \log_2 \left( 1 + \beta |\widehat{h}|^2 \right) \right]$  by a transformation of random variables of the form  $\text{Re}(\widehat{h}) = r \cos(\theta)$ ,  $\text{Im}(\widehat{h}) = r \sin(\theta)$  results in

$$I_{tr} \geq \left( 1 - \frac{1}{N_c} \right) \cdot \log_2(e) \cdot e^{\frac{1}{\beta\sigma^2}} \int_{\frac{1}{\beta\sigma^2}}^\infty \frac{e^{-t}}{t} dt \quad (72)$$

While (72) provides a closed-form lower bound for  $I_{tr}$ , we need a more tractable estimate for the same. For this, we use (68) [24, 5.1.20, pp.229]. Thus  $I_{tr}$  can be further lower bounded as

$$I_{tr} \geq \widehat{I}_{tr} \triangleq \frac{1}{2} \log_e(1+2\beta\sigma^2). \quad (73)$$

This completes the proof of the lemma. ■

### C. Proof of Lemma 2

Since  $\log(\cdot)$  is a monotonically increasing function, the tightest lower bound to  $I_{tr}$  is obtained by maximizing  $K(\eta)$ . A tedious, but straightforward, computation shows that for any  $a, b > 0$ , the function  $f(\eta, a, b)$  defined on  $\eta \in [0, 1]$  as

$$f(\eta, a, b) = \frac{\eta(1-\eta)}{a+b(1-2\eta+\eta N_c)} \quad (74)$$

is concave as a function of  $\eta$ . Now note that  $K(\eta) = N_c^2 \text{SNR}^2 f(\eta, N_c-1, N_c \text{SNR})$ . Thus  $K(\eta)$  is maximized by setting its first derivative to zero.

It is easy to check that the  $\eta$  that is sought is a root of the quadratic

$$\begin{aligned} \eta^2 (N_c \text{SNR} (N_c - 2)) + 2\eta (N_c \text{SNR} + (N_c - 1)) \\ - (N_c \text{SNR} + (N_c - 1)) = 0 \end{aligned}$$

and is precisely  $\eta^*$  as in (30). Using this value of  $\eta^*$  yields the optimal  $K^*$  as in (31). Thus the lemma has been established. ■

### D. Proof of Theorem 1

Substituting  $N_c = \frac{1}{\text{SNR}^\mu}$  in (31), we have

$$\begin{aligned} K^* &= K_1 K_2, \quad K_1 = \frac{\text{SNR}^\mu (\text{SNR} + 1 - \text{SNR}^\mu)}{(1 - 2\text{SNR}^\mu)^2} \\ K_2 &= \left[ \sqrt{1 + \frac{\text{SNR}^{1-\mu} (1 - 2\text{SNR}^\mu)}{\text{SNR} + 1 - \text{SNR}^\mu}} - 1 \right]^2. \end{aligned} \quad (75)$$

We study the low SNR asymptotics of  $K$  for the following four cases – Case 1:  $\mu = 1$ , Case 2:  $\mu \in (1, 3)$ , Case 3:  $\mu \geq 3$  and Case 4:  $\mu < 1$ .

Case 1: It is not difficult to check that

$$K_1 = \text{SNR} + \mathcal{O}(\text{SNR}^2)$$

$$K_2 = \left( \sqrt{2 + \mathcal{O}(\text{SNR}) + \mathcal{O}(\text{SNR}^2)} - 1 \right)^2 = \mathcal{O}(1).$$

Using the above relationships in (32), we see that the coefficient of the SNR-term in the low SNR expansion of  $\hat{I}_{tr}$  is strictly smaller than  $\log_2(e)$ . Thus, first-order optimality fails.

Case 2: When  $\mu \in (1, 3)$ , we have

$$K_1 = \text{SNR}^\mu \sum_{i=\{0,1\}} \sum_{j=0}^{\infty} \mathcal{O}(\text{SNR}^{i+j\mu}) \quad (76)$$

$$K_2 = \frac{1}{\text{SNR}^{\mu-1}} \left[ 1 + 2 \text{SNR}^{\mu-1} - \text{SNR} - 2 \text{SNR}^{\frac{\mu-1}{2}} - \text{SNR}^{\frac{3\mu-3}{2}} + \left(\frac{1}{2}\right)^2 \text{SNR}^{2\mu-2} \right] \quad (77)$$

which implies that one of the  $\text{SNR}^\mu$ ,  $\text{SNR}^{\frac{\mu+1}{2}}$ ,  $\text{SNR}^{\frac{3\mu-1}{2}}$ ,  $\text{SNR}^{2\mu-1}$  terms in  $K$  leads to failure of second-order optimality condition. In particular, the coefficient of the  $\text{SNR}^{1+\epsilon}$  term in (34) is obtained from the coefficient of the  $\text{SNR}^{\frac{\mu-1}{2}}$  term within the parenthesis in (77). However, we get exact first-order optimality in this case.

Case 3: When  $\mu \geq 3$ ,  $K_1$  and  $K_2$  are given by (76) and (77), respectively and every vanishing term is of the form  $\text{SNR}$  or  $\text{SNR}^\nu$  for some  $\nu \geq 2$ . When  $\mu = 3$ , we note that the contribution to the coefficient of the  $\text{SNR}^2$  term can be obtained from (76), (77) and equals  $-3$ . When  $\mu > 3$ , it is easy to see that we get exact second-order optimality. Thus a low SNR expansion of  $\hat{I}_{tr}$  in the form we seek is achievable.

Case 4: When  $\mu < 1$ ,  $K_1$  is given by the same relationship as in (76). But for  $K_2$  we have

$$K_2 = \left( \frac{1}{2} \text{SNR}^{1-\mu} \sum_{i=0}^{\infty} \sum_{j=0}^{\infty} \mathcal{O}(\text{SNR}^{i+j\mu}) \right)^2. \quad (78)$$

This results in the failure of the first-order optimality condition since the largest power of SNR in the Taylor's series expansion of  $\hat{I}_{tr}$  is  $\text{SNR}^{2-\mu}$ . ■

### E. Proof of Theorem 2

We follow the same technique as in Theorem 1. We rewrite the expression for  $\eta^*$  in (30) (using  $N_c = \frac{1}{\text{SNR}^\mu}$ ) as

$$\begin{aligned} \eta^* &= \eta_1 \eta_2, \quad \eta_1 = \frac{\text{SNR}^{\mu-1}(\text{SNR}+1-\text{SNR}^\mu)}{(1-2\text{SNR}^\mu)} \\ \eta_2 &= \left[ \sqrt{1 + \frac{\text{SNR}^{1-\mu}(1-2\text{SNR}^\mu)}{\text{SNR}+1-\text{SNR}^\mu}} - 1 \right]. \end{aligned} \quad (79)$$

To characterize the behavior of  $\text{MSE} = \frac{1}{1+E_{tr}}$ , we analyze  $E_{tr} = \eta^* N_c \text{SNR} = \text{SNR}^{1-\mu} \eta_1 \eta_2$ . We consider the asymptotics in either of the following two scenarios: (i) fixed  $\mu$  and  $\text{SNR} \rightarrow 0$  (as would be the case if we increase  $W$  and scale  $T$  appropriately, according to (18)) (ii) fixed low SNR ( $\ll 1$ ) and increasing  $\mu$  (for large but fixed  $W$  and increasing  $T$ ). The analysis is done over the following three cases: Case 1:  $\mu < 1$ , Case 2:  $\mu = 1$  and Case 3:  $\mu > 1$ .

Case 1: When  $\mu < 1$ , we have

$$\eta_1 = \text{SNR}^{\mu-1} \sum_{i=\{0,1\}} \sum_{j=0}^{\infty} \mathcal{O}(\text{SNR}^{i+j\mu}) \quad (80)$$

$$\eta_2 = \frac{1}{2} \text{SNR}^{1-\mu} \sum_{i=0}^{\infty} \sum_{j=0}^{\infty} \mathcal{O}(\text{SNR}^{i+j\mu}). \quad (81)$$

This leads to

$$\begin{aligned} \eta^* &= \frac{1}{2} + \sum_{i=0}^{\infty} \sum_{j=2}^{\infty} \mathcal{O}(\text{SNR}^{i+j\mu}) \\ E_{tr} &= \frac{1}{2} \text{SNR}^{1-\mu} + \sum_{i=1}^{\infty} \sum_{j=1}^{\infty} \mathcal{O}(\text{SNR}^{i+j\mu}) \end{aligned} \quad (82)$$

which implies that  $\eta^* \rightarrow \frac{1}{2}$  and  $\text{MSE} \rightarrow 1$  (since  $E_{tr} \rightarrow 0$ ).

Case 2: When  $\mu = 1$

$$\begin{aligned} \eta_1 &= 1 + \mathcal{O}(\text{SNR}) \\ \eta_2 &= \sqrt{2 + \mathcal{O}(\text{SNR}) + \mathcal{O}(\text{SNR}^2)} - 1. \end{aligned} \quad (83)$$

The above relationships imply that  $\eta^* \rightarrow 0.414$  and  $\text{MSE} \rightarrow 0.707$ .

Case 3: For  $\mu > 1$ ,  $\eta_1$  is the same as in (80) but the asymptotic expansion for  $\eta_2$  is

$$\eta_2 = \text{SNR}^{\frac{1-\mu}{2}} - 1 + o(1). \quad (84)$$

It is easy to see in this case that  $\eta^* \rightarrow 0$ . Similarly it follows that  $E_{tr} \rightarrow \infty$  and so  $\text{MSE} \rightarrow 0$ . Furthermore, the rates of convergence in this case can be obtained using (80) and (84) and is as illustrated in (39). ■

### REFERENCES

- [1] A. F. Molisch, "Ultrawideband Propagation Channels - Theory, Measurement and Modeling," *IEEE Trans. Veh. Tech.*, vol. 54, no. 5, pp. 1528–1545, Sept. 2005.
- [2] J. Karedal, S. Wyne, P. Almers, F. Tufvesson, and A. F. Molisch, "Statistical Analysis of the UWB Channel in an Industrial Environment," *IEEE Veh. Tech. Conf. (Fall) 2004*, pp. 81–85, 2004.
- [3] C. C. Chong, Y. Kim, and S. S. Lee, "A Modified S-V Clustering Channel Model for the UWB Indoor Residential Environment," *IEEE Veh. Tech. Conf. (Spring) 2005*, 2005.
- [4] A. M. Sayeed and V. V. Veeravalli, "Essential Degrees of Freedom in Space-Time Fading Channels," *Proc. 13th IEEE Intern. Symp. Pers. Indoor, Mobile Radio Commun.*, vol. 4, pp. 1512–1516, Sept. 2002.
- [5] A. M. Sayeed and B. Aazhang, "Joint Multipath-Doppler Diversity in Mobile Wireless Communications," *IEEE Trans. Commun.*, pp. 123–132, Jan. 1999.
- [6] K. Liu, T. Kadous, and A. M. Sayeed, "Orthogonal Time-Frequency Signaling over Doubly Dispersive Channels," *IEEE Trans. Inform. Theory*, vol. 50, no. 11, pp. 2583–2603, Nov. 2004.
- [7] S. Verdú, "Spectral Efficiency in the Wideband Regime," *IEEE Trans. Inform. Theory*, vol. 48, no. 6, pp. 1319–1343, June 2002.
- [8] L. Zheng, M. Medard, and D. N. C. Tse, "Channel Coherence in the Low SNR Regime," *Submitted, IEEE Trans. Inform. Theory*, 2005.
- [9] A. F. Molisch et al., "A Comprehensive Standardized Model for Ultrawideband Propagation Channels," *IEEE Trans. Antennas Propagat.*, vol. 54, no. 11, pp. 3151–3166, Nov. 2006.
- [10] D. Porrat and D. N. C. Tse, "Bandwidth Scaling in Ultrawideband Communication," *Allerton Conf. Commun. Cont. and Comp.*, 2003.
- [11] W. Kozek, *Adaptation of Weyl-Heisenberg Frames to Underspread Environments*, in *Gabor Analysis and Algorithm: Theory and Applications*, H. G. Feichtinger and T. Strohmer, Eds. Boston, MA, Birkhäuser, pp. 323-352, 1997.
- [12] R. S. Kennedy, *Fading Dispersive Communication Channels*, Wiley InterScience, NY, 1969.
- [13] C. C. Chong and S. K. Yong, "A Generic Statistical-Based UWB Channel Model for High-Rise Apartments," *IEEE Trans. Antennas Propagat.*, vol. 53, no. 8, pp. 2389–2399, Aug. 2005.
- [14] R. Saadane, D. Aboutajdine, A. M. Hayar, and R. Knopp, "On the Estimation of the Degrees of Freedom of Indoor UWB Channel," *IEEE Veh. Tech. Conf. (Spring)*, 2005.

- [15] B. Hassibi and B. Hochwald, "How Much Training is Needed in a Multiple Antenna Wireless Link?," *IEEE Trans. Inform. Theory*, vol. 49, no. 4, pp. 951–964, Apr. 2003.
- [16] Í. E. Telatar and D. N. C. Tse, "Capacity and Mutual Information of Wideband Multipath Fading Channels," *IEEE Trans. Inform. Theory*, July 2000.
- [17] L. H. Ozarow, S. Shamai (Shitz), and A. Wyner, "Information Theoretic Considerations for Cellular Mobile Radio," *IEEE Trans. Veh. Tech.*, vol. 43, pp. 359–378, May 1994.
- [18] R. G. Gallager, *Information Theory and Reliable Communication*, John Wiley and Sons Inc., 1968.
- [19] G. Hariharan and A. M. Sayeed, "Minimum Probability of Error in Sparse Wideband Channels," *44th Annual Allerton Conference on Communication, Control and Computing*, Sep. 2006.
- [20] S. Borade and L. Zheng, "Wideband Fading Channels with Feedback," *Allerton Conf. Commun. Cont. and Comp.*, 2004.
- [21] M. Agarwal and M. Honig, "Wideband Channel Capacity with Training and Partial Feedback," *Allerton Conf. Commun. Cont. and Comp.*, 2005.
- [22] C. Carbonelli, S. Vedantam, and U. Mitra, "Sparse Channel Estimation with Zero-Tap Detection," *Proc. IEEE ICC 2004*, 2004.
- [23] I. S. Gradshteyn and I. M. Ryzhik, *Table of Integrals, Series, and Products*, Academic Press, NY, 4th edition, 1980.
- [24] M. Abramowitz and I. A. Stegun, *Handbook of Mathematical Functions with Formulas, Graphs and Mathematical Tables*, National Bureau of Standards, USA, 10th edition, 1972.
- [25] M. Medard, "The Effect Upon Channel Capacity in Wireless Communications of Perfect and Imperfect Knowledge of the Channel," *IEEE Trans. Inform. Theory*, vol. 46, no. 3, pp. 935–946, May 2000.